International Journal of Applied Engineering Research ISSN 0973-4562 Volume 13, Number 7 (2018) pp. 5370-5377

Numerical Simulation of Fatigue Crack Propagation in a Steel Railway Wheel

A. Nebgui,
PhD Student,
Department of Physics,
LEM2A team, Faculty of Sciences-Meknès
Moulay Ismaïl University, Meknès, Morocco.

A. El Kinani,
PhD,
Department of Physics,
LEM2A team, Faculty of Sciences-Meknès
Moulay Ismaïl University, Meknès, Morocco.

M. Haterbouch,
Professor,
Department of Materials and Manufacturing Processes,
M2I team, ENSAM-Meknès
Moulay Ismaïl University, Meknès, Morocco.

O. Oussouaddi,
Professor,
Department of Physics,
LEM2A team, Faculty of Sciences-Meknès
Moulay Ismaïl University, Meknès, Morocco.

A. Zeghloul,
Professor,
LEM3 UMR CNRS N°7239,
Lorraine University, Metz, France.

Abstract

The objective of this paper is to study the influence of the loading intensity and the crack parameters (length and depth) on the fatigue crack propagation rate in a steel railway wheel. The fatigue crack propagation rate is determined by considering that the physical process of propagation is governed by the local damage in the tip of the crack. The values of the stress intensity factors KI and KII have been calculated by using an elastic analysis. The problem has been studied by the aid of the Finite Element Method (FEM) under the hypothesis of plane deformation state. The load, assumed in the form of a moving Hertzian contact pressure, is applied by using a user DLOAD subroutine which has been implemented in the FEM commercial code Abaqus/Standard.

Keywords: Rolling contact fatigue, railway wheel, crack propagation, FEM.

INTRODUCTION

Nowadays, the main objectives of industries are the production of goods with best quality, competitive prices, and ensuring the safety of the parts and guarantee their efficiency. In this context, the materials choice is of particular importance as the mastering of the part lifetime. Mechanical parts are often intended for applications and long term use. In order to have an optimum use, the material must meet a set of criteria: hardness, fracture limit, endurance limit, etc.

Structures such as the wheel and the rail of railway train parts are subjected to cyclic loading that cause, overtime, their fracture: it is the process of fatigue damage. Despite the progresses made in the development of steel production processes and in the manufacture of wheels and rails, they inevitably contain defects that are generally privileged sites for the initiation of fatigue cracks that could reduce the lifetime of these railway components. It is therefore essential to take account of the fatigue strength in the design and manufacture of such structures.

Several authors have studied the behavior of cracks in the two-dimensional case by considering a half-plane subjected to a Hertzian pressure distribution due to the contact between two cylinders with parallel axes and regarding the effect of friction. For example, Kerr et al. [1] and Bastias et al. [2] studied the crack propagation direction. Komvopoulos and Cho [3] developed a two-dimensional finite element model to calculate the stress intensity factors of subsurface cracks and determined approximately the direction of propagation of such cracks under contact loading. Lundén [4] developed three-dimensional models to predict crack propagation in a wheel / rail system by considering the contact between the crack faces.

The propagation of fatigue cracks is generally studied by means of an elastic analysis. However, this approach is based on a stress criterion, while the physical process of propagation is governed by the local damage in the crack tip mainly due to the cyclic strain amplitude suffered [5]. To account of the physical process of propagation, McClintock [6] proposed that the propagation of the crack is due to the accumulation of damage in an area around the crack tip until sudden fracture. The size of this area of activity is taken as a fraction of the cyclic plastic zone. Other authors have also used a similar approach by considering that the average distance between inclusions [7] or the size of a grain [8] as the smallest element of matter for which a failure criterion obtained from a macroscopic law can be applied to.

In this work, the rate of crack propagation in a railway wheel is calculated by taking into account the fact that the physical process of propagation is governed by the local damage at the crack tip. The combined effects of fatigue loading with constant amplitude and involving the modes I and II on the fatigue behavior are considered.

SIMULATION OF THE MECHANICAL BEHAVIOR UNDER CYCLIC LOADING

Description of the wheel / rail contact and the finite element model

According to the classical Hertz contact theory, the rolling contact between the wheel and the rail can be simplified as a two-dimensional plane strain problem.

The finite element software Abaqus/Standard was employed to solve the rolling contact fatigue problem. Figure 1 shows the finite element discretization of a part of a railway wheel containing a crack of length ℓ located at a depth h below the rolling contact surface. The mesh is very fine and dense in the vicinity of the crack tips and becomes gradually radiant when we move away from the crack. Eight-noded biquadratic quadrilateral 2D solid plane strain elements with reduced integration (Abaqus CPE8R) are used in most of the area, but triangular elements of type CPE6M are introduced in the mesh structure, away from the crack, to reduce the total number of elements in order to minimize the simulation time [9]. About 32000 elements are necessary to obtain the numerical convergence according to the loading used.

The normal pressure load is assumed to be elliptically distributed over a contact length of $2b_1$ and translates in the x direction.

The normal pressure distribution on the contact surface is expressed by [10]:

$$p(x) = p_0\sqrt{1-\frac{x^2}{b_1^2}} \qquad (1)$$

with the maximum Hertzian contact pressure given by:

$$p_0 = \sqrt{\frac{FE}{\pi r(1-\nu^2)}} \qquad (2)$$

where F is the normal force per unit length (MN/m), r is the radius of the railway wheel, E and ν are the Young's modulus and Poisson's ratio of the wheel steel, respectively.

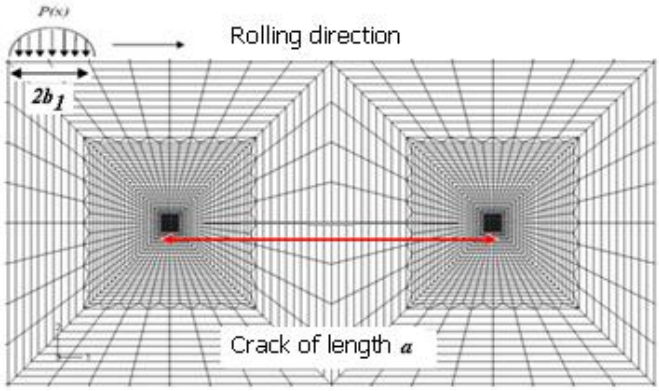

Figure 1: Finite element mesh of the model of a railway wheel with a crack

Material model

A prediction of a reasonable lifetime using a multiaxial fatigue criterion requires a precise knowledge of the state of stress and strain in the steel railway wheel. Hence, in this study we used the nonlinear isotropic/kinematic hardening model proposed by Lemaitre and Chaboche [11]. This model can reproduce various phenomena, such as ratchetting and cyclic hardening caused by repeated rolling contact loading [12-15].

An additive decomposition of the strain rate tensor $\dot{\varepsilon}$ is assumed such that:

$$\dot{\varepsilon} = \dot{\varepsilon}^{el} + \dot{\varepsilon}^{pl} \qquad (3)$$

Where $\dot{\varepsilon}^{el}$ and $\dot{\varepsilon}^{pl}$ represent the elastic and plastic components of the strain rate tensor, respectively.

The pressure-independent yield surface is defined by the function:

$$f(\sigma - X) - R - \sigma^0 = 0 \qquad (4)$$

Where σ is the second-order Cauchy stress tensor, $f(\sigma - X)$ is the equivalent Mises stress potential with respect to the backstress X, σ^0 is the initial yield stress at zero plastic strain and R is the isotropic hardening variable. The equivalent Mises stress potential is defined as:

$$f(\sigma - X) = \sqrt{\frac{3}{2}(S - X') : (S - X')} \qquad (5)$$

where X' is the deviatoric part of the backstress and S is the deviatoric Cauchy stress tensor.

The flow rule is given by:

$$\dot{\varepsilon}^{pl} = \frac{\partial f(\sigma - X)}{\partial \sigma}\dot{\varepsilon}^{pl} \qquad (6)$$

where $\dot{\varepsilon}^{pl}$ represents the rate of plastic flow and $\dot{\bar{\varepsilon}}^{pl}$ is the equivalent plastic strain rate defined as:

$$\dot{\bar{\varepsilon}}^{pl} = \sqrt{\frac{2}{3}\dot{\varepsilon}^{pl} : \dot{\varepsilon}^{pl}} \qquad (7)$$

A common approach for time-independent plasticity uses the decomposition of hardening into kinematic and isotropic parts. These models contain a von Mises yield function and evolution laws for the internal state variables, i.e. the yield stress σ_y, which defines the radius of the elastic range (Mises cylinder), and the backstress tensor X, which describes the shift of the Mises cylinder in the principal stress space.

The isotropic hardening component of the model defines the equivalent stress as a function of the equivalent plastic strain:

$$\dot{R} = b\left(Q - R\right)\dot{\bar{\varepsilon}}^{pl} \qquad (8)$$

where Q and b are the hardening parameters. Q defines the maximum change in the size of the elastic range and b the rate at which the elastic range develops.

When the initial value of *R* is equal to zero, integrating Eq. (8) gives the current yield stress:

$$\sigma_y = \sigma^0 + Q\left(1 - e^{-b\bar{\varepsilon}^{pl}}\right) \qquad (9)$$

The evolution of the kinematic component of the model is based on the Armstrong and Frederick [16] kinematic hardening rule in which the evolution equation for the backstress $\dot{X}$, is given as follows:

$$\dot{X} = \frac{2}{3}C\dot{\varepsilon}^{pl} - \gamma X\dot{\bar{\varepsilon}}^{pl} \qquad (10)$$

C is a hardening modulus and γ defines the rate at which the kinematic hardening modulus decreases as plastic deformation develops. This law is defined as an additive combination of a linear term and a relaxation term, which introduces the non-linearity.

The material parameters of this model are given in Table 1.

Table 1: Material parameters of the Chaboche model for the wheel steel [12].

Parameter	σ^0 $[MPa]$	b	Q $[MPa]$	C $[MPa]$	γ
Value	543	0.47	22.8	6490	0.81

Damage criterion

The models used to treat fatigue damage are divided into two broad categories: those that quantify the damage by using a distortion or an equivalent energy, and those that associate fatigue with a particular plan of fracture or critical plane. The models based on both the energy density and the notion of the critical plane consider that the energy density is the damage parameter to be considered. This parameter is determined on each plane of the material and for each load increment. In this work, a parameter of damage due to Sehitoglu and Jiang [17] is used. This parameter is given by the following equation:

$$FP = \left\langle \sigma_{\max} \right\rangle \frac{\Delta\varepsilon}{2} + J\Delta\tau\Delta\gamma \qquad (11)$$

Where $\langle\ \rangle$ denotes the McCauley bracket, $\langle x \rangle = \frac{1}{2}\left(|x| + x\right)$; $\Delta\varepsilon$ is the normal strain range, $\sigma_{\max}$ is the maximum normal stress; $\Delta\gamma$ is the shear strain range, $\Delta\tau$ is the shear stress range and J is a material and load dependent constant.

All the stress and strain quantities in Eq. (11) are on the critical plane where the fatigue parameter FP, is maximum. Through a tensor rotation for the stresses and strains, $FP_{\max}$ and the corresponding critical plane are determined by surveying all the possible planes at a material point. The weighting parameter *J* is introduced because the mode II of fracture (plane shearing mode) is less damaging than the mode I (opening mode). The Smith-Watson-Topper (SWT) [18] model used to determine the number of cycles to failure is given by:

$$FP_{\max} = \frac{\sigma_f'^2}{E}(2N_f)^{2b'} + \sigma_f'\,\varepsilon_f'\,(2N_f)^{b'+c'} \qquad (12)$$

Where *E* is the elastic modulus; σ_f' and ε_f' are the axial fatigue strength and the axial fatigue ductility coefficients; b' and c' are the fatigue strength and the fatigue ductility exponents.

The mechanical properties for the considered steel grade used in the numerical simulations are presented in Table 2.

Table 2: Mechanical properties for the wheel steel (A.Ekberg, 2001) [19].

E (GPa)	ν	b'	c'	ε_f' (%)	σ_f' (MPa)
210	0.29	-0.089	-0.559	10.3	936

During the propagation of a fatigue crack, the elements located on the crack front are characterized by a continuous increase of the plastic deformation amplitudes that lasts up to failure. Cumulative damage during fatigue is often determined using the earliest, and still most successful rule introduced by Palmgren-Miner. This rule assumes that the total life of a part

can be estimated by adding up the percentage of life consumed by each stress level [5].

The damage in the elements is given by:

$$d_i(\varepsilon_i) = \frac{n_i(\varepsilon_i)}{N_f(\varepsilon_i)} \qquad (13)$$

Here n_i and N_f are the number of applied cycles and the total cycles to fracture, under a plastic deformation level ε_i, respectively.

Taking a linear cumulative damage law (Miner's rule), the propagation of the crack takes place when:

$$\sum d_i = \sum \frac{n_i(\varepsilon_i)}{N_f(\varepsilon_i)} = 1 \qquad (14)$$

The approach based on Miner's rule should be used with caution since it induces a fatigue linear cumulative damage. In the case of sequential tests consisting of two imposed strain levels, this rule overestimates the lifetime when the first cycling sequence is made at the most damaging level [5] due to localized strain hardening. It is, however, much more satisfactory when cycling sequence in the least damaging level is applied first.

By neglecting the variations of the amplitude of the stress intensity factor ΔK, which is equivalent to consider that the rate of propagation of the crack da/dN is constant, one can write:

$$n_i(\varepsilon_i) = \frac{dX_i(\varepsilon_i)}{da/dN} \qquad (15)$$

$dX_i(\varepsilon_i)$ is the width of the element undergoing deformation amplitude ε_i. By summing over all strain levels, we obtain:

$$\frac{da}{dN} = \sum_i \frac{dX_i(\varepsilon_i)}{N_f(\varepsilon_i)} \qquad (16)$$

Therefore, the rate of propagation of the fatigue crack is related to the width of elements located in the tip of the crack and the number of cycle to fracture by:

$$\frac{da}{dN} = \sum_{X=0}^{R_p} \frac{\Delta X}{N_f(\varepsilon)} \qquad (17)$$

Where R_p is the dimension of the cyclic plastic zone, X is the distance to the fracture tip and ΔX is the width of the element for which the finite element calculation gives the amplitude of the equivalent deformation ε after a cycle of loading. $N_f(\varepsilon)$ is calculated by equation (12).

RESULTS AND DISCUSSION

Influence of the loading level

In order to study the influence of the loading level, we consider the case of a horizontal crack of length $\ell = 3$ mm located at a depth $h = 3$ mm and subjected to different Hertzian loads F (0.25, 0.5, 1.0, 2.0, 3.0, 4.0 and 7.0 MN/m). The values of the stress intensity factors K_I and K_{II} are determined by performing an elastic analysis. To achieve the numerical convergence, the size of the elements used is taken equal to 10 μm.

Figure 2 shows the variations of the stress intensity factors K_I and K_{II} as a function of the applied loads. It can be seen that the sliding mode II is more predominant than the opening mode I.

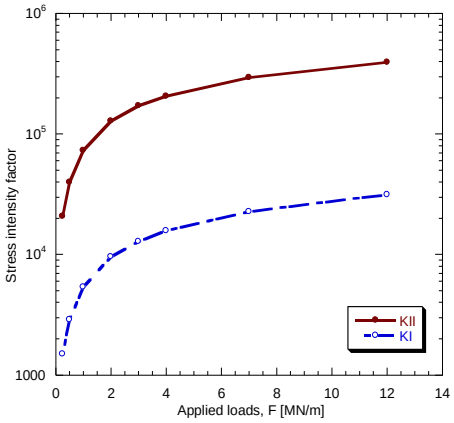

Figure 2: Variation of the mode I and mode II stress intensity factors K_I and K_{II} with the applied load

The variation of the crack growth rate per cycle of loading da/dN as a function of the applied load is represented in Figure 3. This figure shows that the rate of propagation of fatigue crack is negligible for a load of 0.25 MN/m, and increases considerably with the load intensity. Each loading sequence permits to determine a point in the propagation curve da/dN - ΔK_{equiv} as shown in Figure 4.

For fracture under mixed-mode loading, an effective stress intensity factor was evaluated as $\Delta K_{equiv} = \sqrt{K_I^2 + K_{II}^2}$.

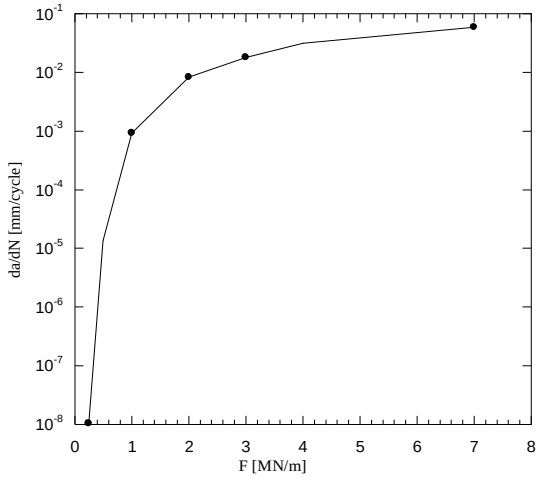

Figure 3: Fatigue crack growth rate as a function of the applied load

For each applied load value, the fatigue crack growth rate is determined at the stabilized cycle. The simulations are done for various values of the applied load varying from 0.25 to 7 MN/m, and hence for the corresponding values of ΔK_{equiv}.

Figure 4 shows that the fatigue crack propagation rate is almost zero for loads less than or equal to 0.25 MN/m. If we consider that the threshold of non propagation of a fatigue crack is defined when the fatigue crack propagation rate is about 10^{-10} (mm /cycle), then the nominal threshold of non propagation of a crack can be set as $\Delta K_{th} = 0.02\ \text{MPa}\sqrt{\text{m}}$.

Influence of the crack depth

In order to analyze the influence of the crack depth on the fatigue crack propagation rate, we consider a crack length equal to $\ell = 3\ \text{mm}$ located at different depths $h = 2,\ 3 \text{ and } 5\ \text{mm}$ and subjected to a Hertzian load F = 0.5 MN/m. In each case, the mesh structure is very fine and dense in the surrounding areas of the crack tips and becomes gradually radiant when we move away from the crack as shown in Figure 5. In the simulations, the width of the elements in the vicinity of the tips is taken equal to 10 μm. More than 61000 elements in the meshing were required for each configuration.

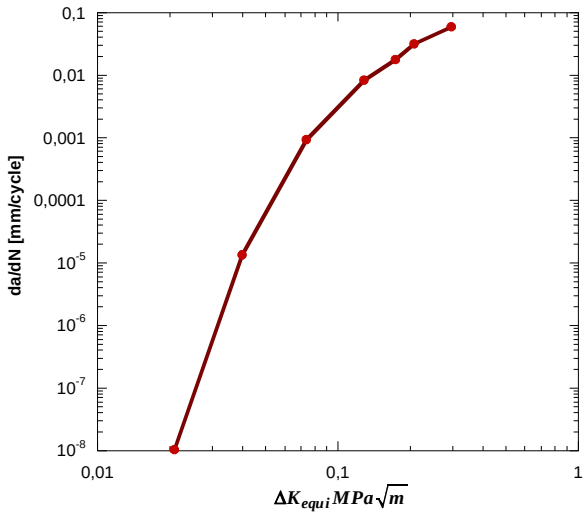

Figure 4: Fatigue crack growth rate as a function of the equivalent stress intensity factor ΔK_{equiv}

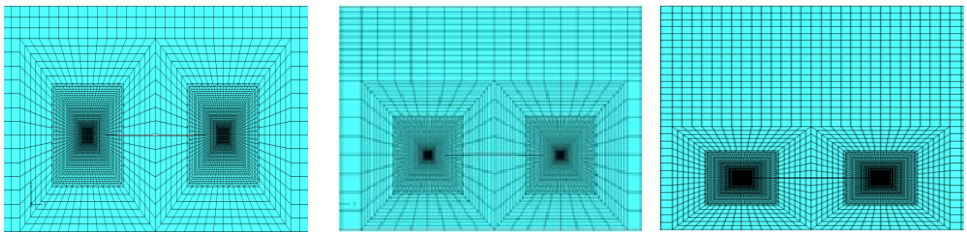

$h = 3$ mm $h = 4$ mm $h = 5$ mm

Figure 5: Meshing structure around the fatigue crack tips for various values of the crack depth

The variation of the rate of propagation of a fatigue crack da/dN with the amplitude of the equivalent stress intensity factor ΔK_{equiv} [MPa.$\sqrt{m}$] is plotted in Figure 6. ΔK_{equiv} was determined in each case by performing linear elastic analysis. It can be seen from this figure that the rate of propagation of a fatigue crack da/dN decreases with increasing values of the equivalent stress intensity factor ΔK_{equiv}.

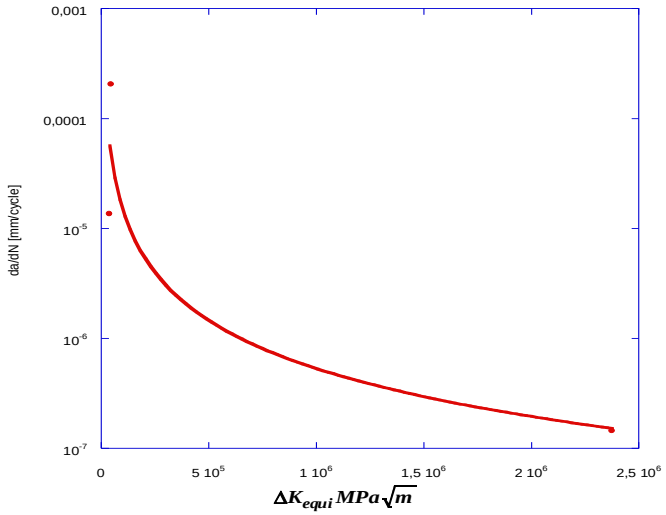

Figure 6: Fatigue crack growth rate da/dN as a function of the equivalent stress intensity factor ΔK_{equiv}, obtained for the various crack depths considered

Influence of the crack length

Cracks located at a depth $h = 3$ mm and having different initial lengths $\ell = 3, 4$ and 5 mm and subjected to a Hertzian load F = 0.5 MN/m are considered here in order to study the influence of the crack length on fatigue crack propagation rate da/dN. Figure 7 shows the meshing used in each case. In our simulations, the size of the elements in the vicinity of the tips is taken equal to 10 μm. The variation of the fatigue crack propagation rate da/dN as a function of the equivalent stress intensity factor ΔK_{equiv}, obtained for different values of the crack depth, is shown in Figure 8.

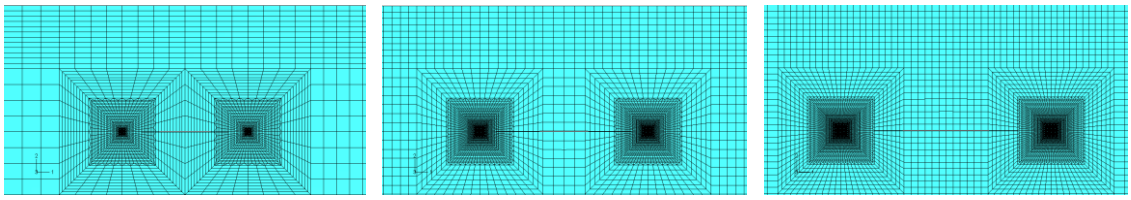

$\ell = 3$ mm $\ell = 4$ mm $\ell = 5$ mm

Figure 7: Meshing structure around the fatigue crack tips for various values of the crack length

It can be seen from this figure that the fatigue crack propagation rate da/dN increases with increasing values of the equivalent stress intensity factor ΔK_{equiv}, i.e., with increasing values of the crack length. Hence, short fatigue cracks propagate slowly compared to long fatigue cracks. This behavior has been related by other authors for different stress amplitudes in the case of 304L stainless steel [20]. However, it must be stressed that short cracks are able to grow below the threshold for long crack growth, and that they can grow

significantly faster than long cracks at the same cyclic stress intensity factor range.

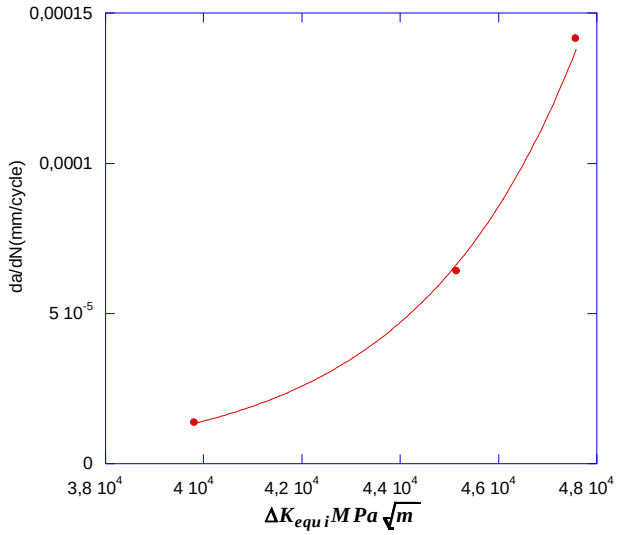

Figure 8: Fatigue crack propagation rate da/dN as a function of the equivalent stress intensity factor ΔK_{equiv} obtained for various crack lengths considered

CONCLUSION

This paper summarizes several important aspects and results related to the subsurface fatigue crack propagation under rolling contact fatigue. Among the results, we performed a parametric study to determine the non-propagation threshold of fatigue cracks. The results obtained in the study allow us to draw the following conclusions:

- Stress intensity factors K_I and K_{II} have been calculated using finite element analysis results under mixed-mode loading conditions in the presence of a crack. We showed that the mode II contribution dominates in comparison with the minor role of the mode I.
- We have shown that the fatigue crack propagation rate greatly increases with the value of the applied load.
- The increase in the equivalent stress intensity factor ΔK_{equiv}, results in a considerable increase in the crack propagation rate.
- The fatigue crack propagation rate decreases sharply when the crack depth varies from 2 to 3 and then decreases more slowly for large depths. Therefore, we concluded that the more the crack is located near the surface, the greater the speed of propagation increases.
- In addition, we have shown that the fatigue crack propagation rate da/dN increases with the crack length. This phenomenon is explained by the decrease in the stress intensity factor of crack tip for the cases studied.

REFERENCES

[1] L. M. Keer, M. D. Bryant, G. K. Haritos, "Subsurface and surface cracking due to Hertzian contact," ASME J. Lubricat. Tech., vol. 104, pp. 347-351, 1982.

[2] P. C. Bastias, G. T. Hahn, C. A. Rubin., "Finite element modeling of subsurface mode II cracks under contact loads," Eng. Fract. Mech., vol. 33, pp. 143-152, 1989.

[3] K. Komvopoulos., S- S. Cho, "Finite element analysis of subsurface crack propagation in a half-space due to a moving asperity contact," Wear, vol. 209, pp. 57-68, 1997.

[4] R. Lundén, "Cracks in railway wheels under rolling contact load," Proceedings of the 10th International Wheelset Congress, Sydney, Australia. pp. 163-167, 1992.

[5] A. Zeghloul, "Comparaison de la propagation en fatigue des fissures courtes et des fissures longues," Thèse de doctorat, ENSMA, Poitiers, France 1988.

[6] F. A. McClintock, "On the plasticity of the growth of fatigue cracks," in Fracture of solids, Interscience Publ., New York, pp. 65-102, 1963.

[7] W. L. Morris, M. R. James, O. Buck, "Computer simulation of fatigue crack initiation," Eng. Fract. Mech., vol. 13, pp. 213-221, 1980.

[8] G. Chalant, L. Remy, "Model of fatigue crack propagation by damage accumulation at the crack tip," Eng. Fract. Mech., vol. 18, pp. 939-952, 1983.

[9] ABAQUS, Inc., ABAQUS User Manual, V6.11-1, 2011

[10] H. Hertz, "On the contact of elastic solids," J. Reine Angew. Math., vol. 92, pp. 156-171, 1881.

[11] A J. Lemaitre, J. L. Chaboche, Mécanique des matériaux solides, Dunod, Paris, 1988.

[12] M. Ekh, A. Johansson, H. Thorberntsson, B.L. Josefson, "Models for cyclic ratchetting plasticity - integration and calibration," Trans. ASME J. Eng. Mater. Technol., vol. 122, pp. 49-55, 2000.

[13] J. W. Ringsberg," Life prediction of rolling contact fatigue crack initiation," Int. J. Fatigue, vol. 23, pp. 575-586, 2001.

[14] M. Abbadi, S. Belouettar, P. Muzzo, P. Kremer, O. Oussouaddi, A. Zeghloul, "On low cycle fatigue life of nickel-based superalloy valve membranes

under non-proportional cyclic loading," Int. J. of Fatigue, vol. 30, pp. 1160-1168, 2008.

[15] M. Taraf, E. H. Zahaf, O. Oussouaddi, A. Zeghloul, "Numerical analysis for predicting the rolling contact fatigue crack initiation in a railway wheel steel," Tribol. Int., vol.4, pp. 585-593, 2010.

[16] P. J. Armstrong, C.O. Frederick, "A Mathematical Representation of the Multiaxial Baushinger Effect," Cegb report rd/b/n731, Berkeley Nuclear Laboratories, 1966.

[17] H. Sehitoglu, Y. Jiang, "Fatigue and stress analyses of rolling contact," College of Engineering, University of Illinois at Urbana-Champaign, Technical Report 161, 1992.

[18] K.N. Smith, P. Watson, T. H. Topper, "A stress–strain function for the fatigue of metals," J. Mater., vol. 5, pp. 767-778, 1970.

[19] A. Ekberg, P. Sotkovszki, "Anisotropy and rolling contact fatigue of railway wheels," Int. J. Fatigue, vol. 23, pp. 29–43, 2001.

[20] A. Soulami, " Modélisation du comportement des aciers 100% austénitiques à transformation de phase. Applications aux calculs des vitesses de propagation en fatigue," Thèse de Doctorat, Université Paul Verlaine de Metz, France, 2006.